

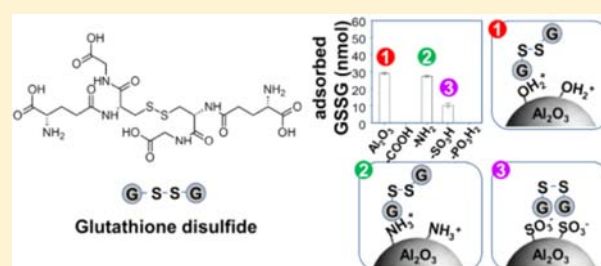
Adsorption and Orientation of the Physiological Extracellular Peptide Glutathione Disulfide on Surface Functionalized Colloidal Alumina Particles

Fabian Meder,^{†,||} Henrik Hintz,^{‡,||} Yvonne Koehler,^{‡,§} Maike M. Schmidt,^{‡,§} Laura Treccani,[†] Ralf Dringen,^{‡,§} and Kurosch Rezwan^{*,†}

[†]Faculty of Production Engineering, Advanced Ceramics, [‡]Center for Biomolecular Interactions Bremen, and [§]Center for Environmental Research and Sustainable Technology, University of Bremen, Bremen, Germany

S Supporting Information

ABSTRACT: Understanding the interrelation between surface chemistry of colloidal particles and surface adsorption of biomolecules is a crucial prerequisite for the design of materials for biotechnological and nanomedical applications. Here, we elucidate how tailoring the surface chemistry of colloidal alumina particles ($d_{50} = 180$ nm) with amino ($-\text{NH}_2$), carboxylate ($-\text{COOH}$), phosphate ($-\text{PO}_3\text{H}_2$) or sulfonate ($-\text{SO}_3\text{H}$) groups affects adsorption and orientation of the model peptide glutathione disulfide (GSSG). GSSG adsorbed on native, $-\text{NH}_2$ -functionalized, and $-\text{SO}_3\text{H}$ -functionalized alumina but not on $-\text{COOH}$ - and $-\text{PO}_3\text{H}_2$ -functionalized particles. When adsorption occurred, the process was rapid (≤ 5 min), reversible by application of salts, and followed a Langmuir adsorption isotherm dependent on the particle surface functionalization and ζ potential. The orientation of particle bound GSSG was assessed by the release of glutathione after reducing the GSSG disulfide bond and by ζ potential measurements. GSSG is likely to bind via the carboxylate groups of one of its two glutathionyl (GS) moieties onto native and $-\text{NH}_2$ -modified alumina, whereas GSSG is suggested to bind to $-\text{SO}_3\text{H}$ -modified alumina via the primary amino groups of both GS moieties. Thus, GSSG adsorption and orientation can be tailored by varying the molecular composition of the particle surface, demonstrating a step toward guiding interactions of biomolecules with colloidal particles.



1. INTRODUCTION

Inorganic colloidal particles become coated with biomolecules like peptides and proteins when exposed to biological fluids.^{1,2} How the particle surface chemistry guides the adsorption and orientation of the biomolecules on the particle surface is yet not well understood but crucial for the tailored design and successful application of submicrometer- and nanoparticles in many biotechnological and nanomedical applications and for toxicological considerations.^{1–3}

Peptide–particle interactions are a model system for the more complex protein–particle interactions and, moreover, important for biosensing applications,⁴ biomineralization,⁵ antibacterial surface modification,⁶ cell–material adhesion,⁷ and controlled drug release.⁸ Peptide adsorption onto particle surfaces are, nevertheless, hard to control as contributions of either electrostatic, hydrophobic interactions or hydrogen bonding,^{9–13} the main driving forces of peptide–particle interactions, are often not fully enlightened.^{2,10,14} However, it is becoming apparent that peptides “recognize” particle surface properties and bind material specific and selective toward different oxide particles.^{15–17} Such peptides with affinity toward a specific material can be obtained by phage display techniques.^{17,18} In contrast, to promote or avoid binding of a given peptide onto an oxide particle, it is necessary to engineer

the particle surface itself with specific properties to induce the desired interaction (attraction/repulsion of the peptide).¹⁹

Surface functionalization allows to tailor the surface properties of colloidal particles and to facilitate the attachment of charged groups (e.g., $-\text{NH}_3^+$, $-\text{SO}_3^-$) onto almost any metal oxide particle. Such particle surface groups can interact with oppositely charged carboxylate or amino groups in peptides.^{9,20–23} However, peptide adsorption deviates from predictions by just considering the net charges of particles and peptides.^{15,21,23} Due the multifunctionality of peptides (e.g., coexistence of cationic and anionic surface groups), it is crucial, but often unclear, which particle functional groups and peptide residues indeed interact on a molecular level during peptide–particle adsorption.

Colloidal alumina particles are an ideal substrate for stable and tunable surface functionalizations^{21,22,24} and thus an appreciated model system to study peptide–particle adsorption as a function of different surface chemistry. Alumina is moreover widely used as a substrate material for biomedical and biotechnological applications, including, e.g., biosensing,²⁵ protein separation and purification systems,²⁶ biocatalysis,²⁷ or

Received: February 13, 2013

Published: April 8, 2013

drug delivery applications.^{28,29} The alumina particle features surface hydroxyl groups (Al–OH) that can be used to functionalize the particle surface with, e.g., –NH₂ or –SO₃H groups. On the other hand, the Al–OH groups are itself positively charged sites on the particle surface when they protonate (Al–OH₂⁺) below the particles' isoelectric point (IEP) of about 9.²²

An important physiological peptide is glutathione disulfide (GSSG; γ -GluCysGly disulfide) that derives from the oxidation of glutathione (GSH; γ -GluCysGly) and is the disulfide of two GSH molecules.¹¹ The GSH/GSSG redox pair is a highly important redox system in eukaryotic cells, and GSH is a necessary molecule in the defense of cells against oxidative stress and toxins.^{30,31} Intact mammalian cells contain hardly any GSSG. In defending oxidative stress, GSH is oxidized to GSSG and then either regenerated by reduction or efficiently exported by multidrug resistance proteins, as shown for various cell types.^{11,32–34} GSSG export helps to prevent a toxic intracellular GSSG surge and leads to substantial extracellular GSSG concentrations, that partially also derive from extracellular GSH oxidation.³² In body fluids, such as blood serum, GSSG concentrations of up to 150 μ M are found.³⁵ Materials that come into contact with serum in biomedical and biotechnological applications thus likely encounter extracellular GSSG. GSSG, as a marker for oxidative stress, is furthermore a targeted peptide in several biosensor applications.^{36,37}

GSSG is an ideal biomolecule for the investigation of the adsorption and desorption behavior on surface functionalized particles. GSSG contains a disulfide bridge in addition to carboxylate and amino groups and has been therefore considered as a suitable model peptide for small proteins and epitopes of larger proteins involved in protein-particle binding.¹¹ In addition, the availability of a specific enzymatic cycling assay for the quantification of picomole amounts of GSSG allows a rapid and highly sensitive determination of even low quantities of GSSG that have adsorbed or desorbed from moderate amounts of particles.³⁸ GSSG adsorption onto native colloidal alumina particles was recently studied by Dringen et al., who found that GSSG strongly adsorbs onto alumina via electrostatic interactions between carboxylate groups of one GSSG moiety and the positively charged alumina surface.¹¹

In this study, we investigate how the GSSG adsorption and orientation on alumina particles can be modulated by tailoring the particle surface with acidic (–COOH, –SO₃H, –PO₃H₂) and basic (–NH₂) surface groups. We have previously shown that such surface functionalizations direct protein adsorption processes.^{21,22} This study goes beyond and here, the GSSG-particle binding mechanisms, contribution of particles and GSSG functional surface groups, and its orientation on the particle surface could be elucidated on a molecular level by studying GSSG adsorption on well-characterized surface functionalized particles in combination with ζ potential measurement and analysis of the GSSG disulfide bond reduction on the particle surfaces. Therefore the results broaden fundamental understanding of protein–surface interactions and are valuable for developing surface design strategies for colloidal particles in biomedical and technological applications.

2. MATERIALS AND METHODS

2.1. Materials. Polycrystalline α -alumina particles (Al₂O₃; TM-DAR, lot. no. 8086, high-purity alumina >99.99%, d_{50} = 179 \pm 8 nm, density = 3.98 g/cm³, specific surface area = 11.5 m²/g) were

purchased from Krahn Chemie (Germany). For surface functionalization we used 3-aminopropyltriethoxysilane (99% in ethanol) for –NH₂ groups and pyrophosphoric acid (\geq 90%) for –PO₃H₂ groups, both from Sigma-Aldrich (Germany). 3-(triethoxysilyl)propylsuccinicanhydride, >94%, was used to generate –COOH groups and 3-(triethoxysilyl)-1-propanesulfonic acid, 30–35% in H₂O for –SO₃H groups, both purchased from ABCR (Germany). 5,5'-dithio-bis(2-nitrobenzoic acid) (DTNB), ethylenediaminetetraacetic acid (EDTA), and GSSG were obtained from Sigma-Aldrich (Germany). Dithiothreitol (DTT), nicotinamide adenine dinucleotide phosphate (NADPH), and sulfosalicylic acid were obtained from AppliChem (Germany). Glutathione reductase was purchased from Roche Diagnostics (Germany). All other chemicals were obtained from Fluka (Switzerland) or Merck (Germany) at analytical grade.

2.2. Methods. 2.2.1. Surface Functionalization of Al₂O₃ Particles.

Alumina particles were functionalized as described previously by Meder et al.²² Briefly, suspensions of α -alumina particles, prepared by mixing 15 g particles with 50 mL double-deionized water (ddH₂O) with an electrical resistance of 18 M Ω \times cm (Synergy, Millipore, Germany), were deagglomerated by sonication for 10 min with an ultrasound horn Sonifier 450 (Branson, U.S.A., output: 150 W, pulse rate: 0.5 s). The precursors were mixed with 50 mL ddH₂O to a final concentration of 0.09 M (this corresponds to 26 μ mol/m², normalized to the specific surface area of the unmodified Al₂O₃ particles). Subsequently, the precursor solution was added to the particle suspensions and stirred for 60 min at 25 $^{\circ}$ C and was then heated for 90 min at 115 $^{\circ}$ C. Afterward, the particles were separated by centrifugation and washed three times in 100 mL ddH₂O to remove any unreacted precursors. Then the particles were freeze-dried for 96 h at –20 $^{\circ}$ C in vacuum using a freeze-dryer P8KE-80 (Piatkowski Forschungsgeräte, Germany) and subsequent heat treated at 70 $^{\circ}$ C for 2 h. The native alumina was calcined at 400 $^{\circ}$ C for 4 h followed by autoclaving for 15 min at 121 $^{\circ}$ C and 2.05 bar (Systec 2540ELV, Systec, Germany) as a sterilization step, according to Dringen et al.¹¹


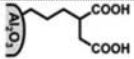
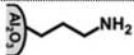
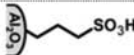
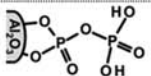
2.2.2. Particle Characterization. The ζ potential measurements were conducted with an electroacoustic spectrometer DT1200 (Dispersion Technology Inc., U.S.A.). Isoelectric points were determined by pH titrations using 1 M HCl or 1 M KOH. All measurements were conducted with suspensions containing 1 vol % of particles. Average and standard deviations were calculated from three independent measurements. This procedure was also used to determine the ζ potential and IEP of particles with GSSG.

Specific surface areas were calculated from nitrogen adsorption isotherms using the Brunauer, Emmet, and Teller (BET) equation. Adsorption isotherms have been recorded at –196 $^{\circ}$ C with an automated surface area analyzer BELSORP-mini (Bel Inc., Japan). All samples were gassed out at 120 $^{\circ}$ C under vacuum for 3 h before the measurement.

Particle size was measured by dynamic light scattering with an Ultrafine Particle Analyzer UPA 150 (Microtrac Inc., USA) using aqueous suspensions with 0.1 vol % particle content. The average and standard deviations were calculated from four to nine single measurements of the d_{50} (intensity).

Elemental analysis was carried out by Mikrolabor Pascher (Germany), and element concentrations were used to calculate the amounts of functional groups related to the specific surface area of unfunctionalized alumina particles (11.5 m²/g). Inductive coupled plasma atomic emission spectroscopy was applied to determine the sulfur and phosphorus content of the functionalized particles after acid pressure hydrolysis in an ICAP 6500 (Thermo, Germany). To quantify the amino groups, the nitrogen content was determined using the Dumas method.³⁹ Carboxylate groups were determined by measuring the carbon concentration by conductometric carbon dioxide determination after combustion. The lower detection limit of the elemental analysis was 0.01 wt % for S, P, and C and 0.1 wt % for N. The analysis was conducted in duplicates. Further characterizations of the functionalized particles including transmission electron microscopy, water vapor, and *n*-heptane adsorption to determine the hydrophilic and hydrophobic properties of the particles can be found in Meder et al.²²

Table 1. Physicochemical Properties of Functionalized and Unfunctionalized Alumina Particles

Surface functionalization and sample name	Functional groups density ($\pm 0.2 \text{ nm}^{-2}$)	Surface area (m^2/g)	d_{50} (nm)	IEP (± 0.2)
 Al_2O_3 unfunctionalized	2.0	11.5	179 ± 8	9.3
 $\text{Al}_2\text{O}_3\text{-COOH}$	4.4	13.3	187 ± 9	3.2
 $\text{Al}_2\text{O}_3\text{-NH}_2$	<3.4	11.8	186 ± 5	11.0
 $\text{Al}_2\text{O}_3\text{-SO}_3\text{H}$	4.6	17.6	174 ± 8	1.5
 $\text{Al}_2\text{O}_3\text{-PO}_3\text{H}_2$	2.3	13.6	180 ± 8	2.4

2.2.3. Incubation of GSSG with the Particles. Aqueous particle suspensions (1 vol %) were prepared by mixing 398 mg particles in 9.9 mL ddH₂O. The suspensions were then deagglomerated for 10 min using an ultrasound horn Sonifier 450 (Branson, U.S.A., output: 150 W, pulse rate: 0.5 s). The as-prepared suspensions were subsequently incubated with GSSG under the conditions indicated for the individual experiments. All incubations were performed at room temperature (25 °C). Particle sedimentation was prevented by permanent mixing using a rotator drive STR4 (Staffordshire, USA) at a speed of 13 rpm (adsorption/desorption experiments) or by using a horizontal shaker Unimax 1011 (Heidolph Instruments, Germany).

For the adsorption experiments, 50 μM GSSG, or the GSSG concentration stated in the figure, was incubated with 0.1 vol % particle suspension in 1 mL ddH₂O. The pH for the prepared suspensions was 4.8 for Al_2O_3 , 6.4 for $\text{Al}_2\text{O}_3\text{-NH}_2$, 4.3 for $\text{Al}_2\text{O}_3\text{-COOH}$, 4.2 for $\text{Al}_2\text{O}_3\text{-SO}_3\text{H}$, and 4.1 for $\text{Al}_2\text{O}_3\text{-PO}_3\text{H}_2$. After different incubation time intervals (60 min or as stated in the figures), the samples were centrifuged for 10 min at 12 100 g (Minispin, Eppendorf, Germany), and the remaining GSSG in the supernatant of the solution was determined.

To quantify the particle bound GSSG, the GSSG was released from the particle surface using a procedure adapted from Dringen et al.¹¹ Therefore, the pellet, received in the above-described centrifugation step, was washed with 1 mL ddH₂O and centrifuged again (5 min, 12 100 g). This pellet was then resuspended in 1 mL 10 mM KOH (pH 12.3) by vortexing and directly centrifuged (10 min, 12 100 g). Incubation of the particles in 10 mM KOH for up to 60 min (as done in the procedure of Dringen et al.)¹¹ did not further increase the amount of released GSSG. The KOH treatment was sufficient to completely release the particle bound GSSG, which was then quantified.

2.2.4. Reduction of Particle Bound GSSG. The disulfide bonds of particle bound GSSG were reduced using DTT. Therefore, 0.1 vol % particle suspensions were preincubated for 30 min with 1 mM GSSG. After centrifugation (10 min at 12 100 g) and washing with 1 mL ddH₂O, the particle pellets were dispersed in 1 mL ddH₂O containing no DTT or 20 mM DTT. After 60 min of incubation, the particles were washed, and the bound GSSG or GSH was released with KOH as described above. The samples for the ζ potential measurements were prepared likewise using a 1 vol % particle suspension to achieve a reliable signal. The concentrations of GSSG and DTT were accordingly upscaled to 10 mM GSSG and 200 mM DTT.

2.2.5. Effect of Ions on Particle Bound GSSG. To investigate the potential of ions to desorb GSSG from the particles, 1 mM GSSG were preincubated with 0.1 vol % particle suspensions for 30 min in 1 mL total volume. After centrifugation (10 min, 12 100 g) the pellet was washed with 1 mL ddH₂O, dispersed in 1 mL ddH₂O or in ddH₂O containing NaCl, Na₂SO₄, or (NH₄)₂SO₄ in concentrations of up to 100 mM and subsequently incubated for 60 min. The pH of the ddH₂O and salt solutions was 6.2. After centrifugation, the supernatant was harvested, and the desorbed GSSG was determined.

2.2.6. Determination of GSSG and GSH. GSSG was quantified as described previously^{40,41} in microtiter plates according to the colorimetric method originally described by Tietze et al.³⁸ Briefly, 10 μL of the supernatant was mixed with 10 μL 1% (w/v) sulfosalicylic acid and diluted with 80 μL ddH₂O in a well of a microtiter plate. The reaction was started by the addition of 100 μL reaction mixture (0.06 U glutathione reductase, 0.3 mM DTNB, 0.4 mM NADPH, 1 mM EDTA in 0.1 M sodium phosphate buffer, pH 7.5), and the increase in absorbance due to the formation of 5-thio-2-nitrobenzoate was followed at 405 nm using a microtiter plate reader (Sunrise, Tecan, Austria). GSSG contents were calculated by comparison to values obtained for GSSG standards. This assay detects GSH in addition to GSSG.³⁸ Therefore, the amount of GSH that was adsorbed to the particles after treatment of GSSG-bound particles with DTT was also quantified by the GSSG assay, considering that a given GSH amount gives only half of the signal of the respective GSSG amount.

2.2.7. Adsorption Isotherm Fit. The experimental adsorption isotherm was fitted using the Langmuir equation:

$$\Gamma = \frac{\Gamma_{\max} * c}{K_L^{-1} + c}$$

where Γ and Γ_{\max} are the adsorbed and maximal adsorbed quantities, respectively, c is the GSSG concentration in solution, and K_L^{-1} is the Langmuir constant of the system. K_L^{-1} was then used to calculate the standard Gibbs energy of adsorption ΔG_{ads}^0 as previously described^{42,43} using the equation:

$$\Delta G_{\text{ads}}^0 = -RT \ln \left(\frac{c_{\text{solv}}}{K_L^{-1}} \right)$$

where R is the gas constant, T is the standard ambient temperature, and c_{solv} is the molar concentration of the solvent water (55.5 mol/L).

2.2.8. Modeling of GSSG Properties. The partial charge distribution of GSSG as function of the pH was calculated from equilibrium constants predicted by linear free energy relationships using ACD/Labs-Lab 2.0, version 5.0.0.184, Advanced Chemistry Development, Inc., Toronto, ON, Canada, www.acdlabs.com.⁴⁴ To calculate the surface potential distribution, the chemical structure information for GSSG available in the PubChem substance and compound database through the substance identifier number CID: 44630308⁴⁵ was used, and Gasteiger partial charges were assigned using Vega ZZ (version 3.0.1).⁴⁶ The GSSG surface potential at neutral pH and ionic strength of 1 mM at 25 °C was calculated using the adaptive Poisson–Boltzmann solver,⁴⁷ and isosurfaces of negative and positive potentials represent equipotentials of ± 30 mV visualized using Visual Molecular Dynamics (version 1.8.7).⁴⁸

3. RESULTS

3.1. Characteristics of Surface Functionalized Particles. Table 1 shows the physicochemical properties of the five

types of colloidal alumina particles investigated in this study. The surface densities of the functional groups after surface functionalization were found between 2.3 and 4.6 ± 0.2 groups/nm² as determined by elemental analysis. The hydroxyl group surface density on native alumina (Al–OH) yields 2.0 ± 0.2 Al–OH/nm² determined by potentiometric titration (data not shown). Comparing the surface densities suggests that on average one precursor molecule associated with one Al–OH group in case of the –COOH and –PO₃H₂ functionalization. During –SO₃H and –NH₂ surface functionalization, a second precursor molecule may additionally condense or cross-link with an already deposited precursor molecule (e.g., via a free silanol group) leading to a functional group density that is about twice than expected from the Al–OH surface density.²¹ The median particle size (d_{50}) was maintained at about 180 nm after surface functionalization (particle size distribution is given in the Supporting Information). The specific surface area determined by nitrogen adsorption slightly increased depending on type and surface density of functional groups attached. This indicates that the small nitrogen molecules can adsorb on the molecules attached to the particle surface increasing the measured particle surface area.²¹ However, these changes of the surface area are expected to be too small to influence the adsorption of a biomolecule like GSSG that is about 10 times larger than a nitrogen molecule. To normalize the GSSG adsorption on the particle surface area (see section 3.4.), thus for all particles, the specific surface area of native Al₂O₃ particles was used. The IEP of native alumina particles was found as expected at pH 9.3⁴⁹ and was shifted toward pH 11 after introduction of the basic –NH₂ groups. In contrast, attachment of acidic –COOH, –PO₃H₂, and –SO₃H groups shifted the IEP to 3.2, 2.4, and 1.5, respectively. A further increase in precursor concentration for functionalization did neither increase the shift of the IEP nor the functional group density (data not shown), suggesting that the conditions used caused a saturation of the particle surface with functional groups. Similar findings are reported in our previous work which shows by transmission electron microscopy that the particle morphology and size are unchanged after surface functionalization and by water vapor and *n*-heptane adsorption studies that the particles have slight differences in their hydrophilic/hydrophobic properties depending on their surface functionalization.²²

3.2. GSSG Structure and pH-Dependent Charge. The GSSG structure is depicted in Figure 1. The charged status of GSSG is strongly affected by the pH which determines the extent of deprotonation and protonation of the carboxyl and amino residues of GSSG (Figure 1). In the pH range of 4–8, which is the pH of the GSSG adsorption experiments, GSSG has a constant total charge of –2 due to four deprotonated carboxylate groups (–COO[–]) and two protonated amino groups (–NH₃⁺). Although GSSG is overall negatively charged, positively charged sites exist, which are illustrated by the surface potential distribution of the GSSG molecule (Figure 1).

3.3. Effect of Surface Functionalization on GSSG Adsorption. Figure 2A depicts the influence of the particle surface functionalization on the amount of GSSG in the supernatant (Figure 2A, left panel) after the particles were incubated with 50 μM GSSG (50 nmol per sample). Figure 2B shows the pH of the as-prepared suspension during GSSG incubation and the ζ potential of the particles at this pH. Incubation with Al₂O₃, Al₂O₃–NH₂, and Al₂O₃–SO₃H significantly reduces the amount of GSSG in the supernatant to 14.2 ± 1.2 , 17.7 ± 0.7 , and 32.6 ± 1.3 nmol, respectively,

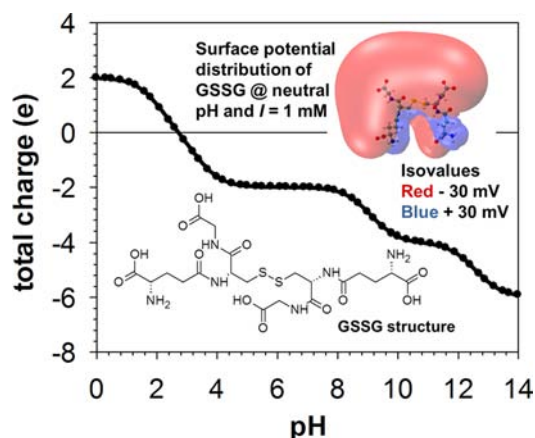


Figure 1. Partial charge distribution of GSSG as function of the pH. Surface potential distribution is represented by isosurfaces of negative (red) and positive (blue) potentials calculated for equipotentials of ± 30 mV at neutral pH and ionic strength of 1 mM at 25 °C.

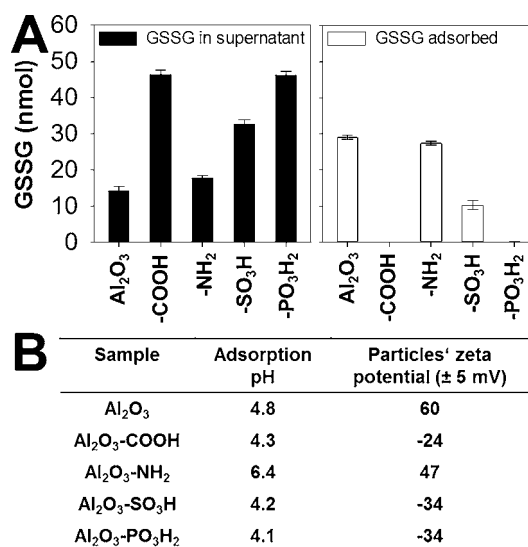


Figure 2. (A) Adsorption of GSSG as function of the surface functionalization of Al₂O₃ particles: 50 nmol GSSG per sample (corresponding to a concentration of 50 μM) was incubated for 60 min with the particles (0.1 vol %) in ddH₂O, and the remaining GSSG content in the supernatant was determined (black bars, left). Subsequently the particles were washed in ddH₂O and resuspended in 10 mM KOH (pH 12.3) to release the adsorbed GSSG (white bars, right). The data represent means \pm standard deviation of three independent experiments. (B) The pH of the as-prepared suspensions during GSSG incubation and the particles' ζ potential at this pH (ionic strength is $\leq 10^{-4}$ M).

indicating GSSG adsorption on these particles. In contrast, none or only marginal GSSG adsorption was found after incubation with Al₂O₃–COOH (46.4 ± 1.3 nmol) or Al₂O₃–PO₃H₂ (46.3 ± 1.2 nmol).

Treatment of the particles after GSSG adsorption with 10 mM KOH enabled to release and quantify the particle bound GSSG (Figure 2A, right panel). For Al₂O₃–COOH and Al₂O₃–PO₃H₂, no GSSG was released by KOH as expected from the, at best, marginal GSSG loss found for the supernatant of these particles. For Al₂O₃, Al₂O₃–NH₂, and Al₂O₃–SO₃H, 29.1 ± 0.6 , 27.4 ± 0.5 , and 10.3 ± 1.0 nmol GSSG were found adsorbed to the particles, respectively, which corresponded well

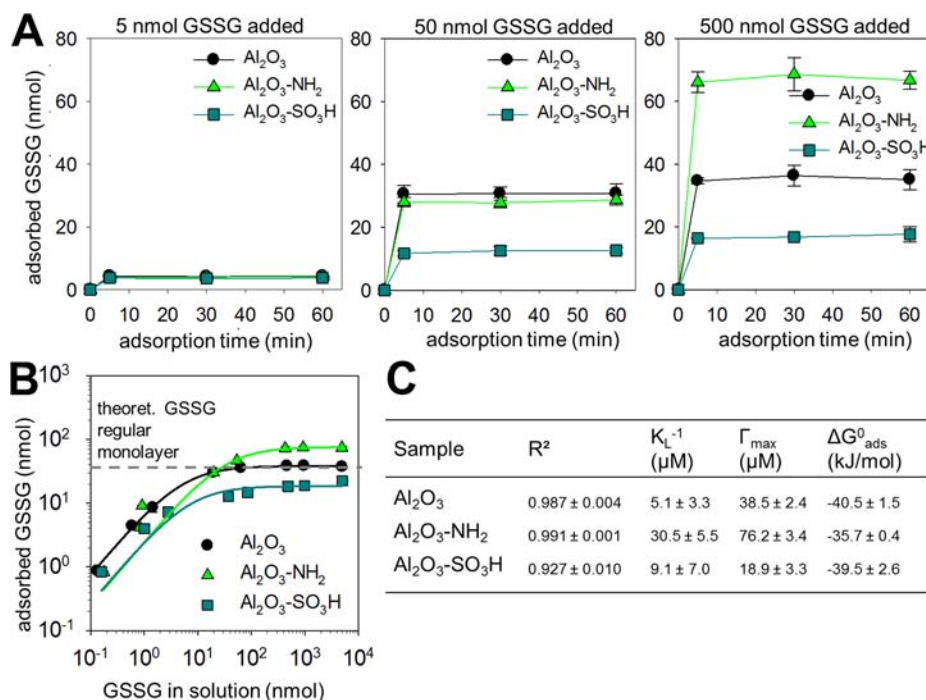


Figure 3. (A) Time and concentration dependency of GSSG adsorption to Al₂O₃, Al₂O₃-NH₂, or Al₂O₃-SO₃H-functionalized particles. The pH for the adsorption phase was 4.8 for Al₂O₃, 6.4 for Al₂O₃-NH₂, and 4.2 for Al₂O₃-SO₃H (at 50 μM GSSG). (B) GSSG adsorption isotherms and Langmuir regressions of the concentration-dependent adsorption of GSSG to Al₂O₃, Al₂O₃-NH₂, or Al₂O₃-SO₃H particles. (C) Langmuir constants and Gibbs energies for the adsorption of GSSG calculated from the values shown in (B). The data shown are the amounts of GSSG that had been released from the particle surface by KOH. The data represent means ± standard deviation of three independent experiments.

with the GSSG loss determined for the supernatant. The KOH treatment partially lowers the amount of particle surface functional groups indicated by IEP measurements (Table S2), and the GSSG release by KOH may be a consequence of alumina particle surface dissolution, dissolution of the functional groups from the particles, and GSSG desorption processes. In fact, the GSSG amounts determined in the KOH supernatants matched the amounts of GSSG that had disappeared from the ddH₂O supernatants, confirming that the KOH treatment of the particles is suitable to quantitatively determine the adsorbed GSSG.

The particle ζ potentials determined for the GSSG adsorption conditions (Figure 2B) indicate that Al₂O₃ and Al₂O₃-NH₂ are, as expected from their IEP (Table 1), net positively charged under the conditions used for GSSG adsorption. Interestingly, among the net negatively charged particles, i.e., Al₂O₃-COOH, Al₂O₃-SO₃H, and Al₂O₃-PO₃H₂, GSSG adsorbed exclusively onto Al₂O₃-SO₃H.

As significant GSSG adsorption was only found on Al₂O₃, Al₂O₃-NH₂, and Al₂O₃-SO₃H, we focused for further analysis on the interaction of GSSG with alumina only on these particle types.

3.4. Time and Concentration Dependencies of GSSG Adsorption. The adsorption of GSSG was found to be rapid and after already <5 min incubation, maximal amounts of GSSG were found adsorbed onto Al₂O₃, Al₂O₃-NH₂, and Al₂O₃-SO₃H that had been incubated with 5, 50, or 500 nmol GSSG (Figure 3A). Longer incubation times of up to 60 min did not result in higher GSSG adsorption, and 30 min adsorption time was used to investigate the concentration dependence of the GSSG binding to Al₂O₃ and Al₂O₃-NH₂- and Al₂O₃-SO₃H-functionalized particles in more detail (Figure 3 B). GSSG adsorption saturated on Al₂O₃ particles

at about 39 μM, which corresponds to 852 nmol GSSG/m² or 1.95 nm²/GSSG molecule when the amount of adsorbed GSSG was normalized to the surface area of the particles. These values correspond quite well to the concentration of a theoretical regular monolayer of GSSG which contains 844 nmol/m² assuming that GSSG occupies a circular surface area of about 1.55 nm² (maximal GSSG projection area,⁵⁰ Figure S3) and a surface packing density of 78.5% (quadratic packing). In case of Al₂O₃-NH₂, GSSG adsorption exceeded a theoretical GSSG monolayer and saturated at about 76 μM (1660 nmol GSSG/m²). The area that one GSSG molecule occupied on Al₂O₃-NH₂ was about 1.0 nm², which corresponds to the theoretical minimal projection area of GSSG of 1.0 nm²⁵⁰ (Figure S3). For Al₂O₃-SO₃H, GSSG adsorption saturated already at about 19 μM (415 nmol GSSG/m² corresponding to an adsorption area of 4.0 nm² per GSSG molecule), which is below the calculated theoretical monolayer.

The Langmuir regression provided a good fit for the adsorption data (Figure 3B). The correlation coefficient and the characteristic Langmuir constants calculated for the GSSG adsorption onto Al₂O₃, Al₂O₃-NH₂ or Al₂O₃-SO₃H particles are given in Figure 3C. The Gibbs energies of GSSG adsorption ΔG_{ads}⁰ were calculated from the Langmuir fits of each particle type and were found similar for Al₂O₃, Al₂O₃-NH₂, and Al₂O₃-SO₃H.

3.5. Desorption of GSSG by Salt Addition. To estimate the contribution of electrostatic interactions in the binding of GSSG to alumina particles, the effect of ions of varying type and valences on the amount of GSSG bound to Al₂O₃, Al₂O₃-NH₂, or Al₂O₃-SO₃H particles was investigated. Particles were preincubated with 1000 nmol GSSG which resulted in maximal binding of GSSG to the particles (Figure 3). Subsequently, the GSSG-loaded particles were incubated with salt solutions of pH

6.2. The relative amount of GSSG desorbed from the particles by different ions is depicted in Figure 4. The presence of NaCl

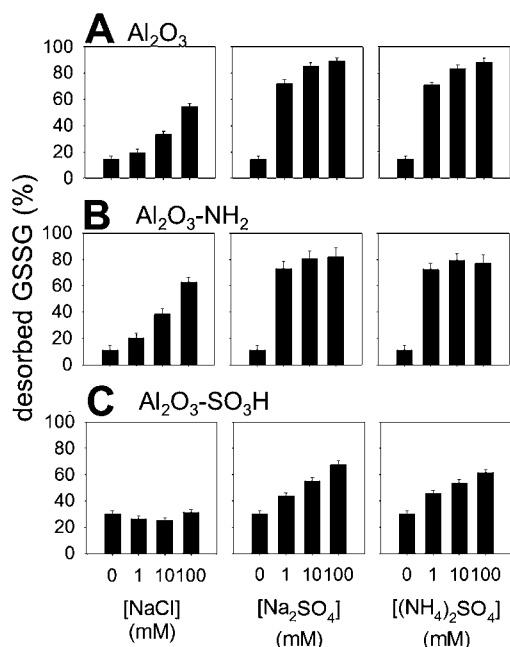


Figure 4. Desorption of GSSG from Al_2O_3 , $\text{Al}_2\text{O}_3\text{-NH}_2$, or $\text{Al}_2\text{O}_3\text{-SO}_3\text{H}$ -functionalized particles resuspended in different salt solutions. The 1000 nmol GSSG was preincubated with 0.1 vol % of the particles for 30 min. Subsequently, particles were centrifuged, washed with 1 mL ddH₂O, resuspended in ddH₂O at pH 6.2 containing NaCl, Na₂SO₄, or (NH₄)₂SO₄ in the indicated concentrations, and incubated for 60 min. The data represent the relative desorbed GSSG amounts. Means \pm standard deviation are of three independent experiments.

leads to a concentration-dependent increase in GSSG desorption from Al_2O_3 and $\text{Al}_2\text{O}_3\text{-NH}_2$ particles. After incubation with 100 mM NaCl, about 55% (Al_2O_3) and 63% ($\text{Al}_2\text{O}_3\text{-NH}_2$) of the bound GSSG had been desorbed. The 1:2 electrolyte Na₂SO₄ resulted at a concentration of 100 mM in a stronger desorption reaching 89% GSSG desorption for Al_2O_3 and 82% for $\text{Al}_2\text{O}_3\text{-NH}_2$. In (NH₄)₂SO₄ solution (also 1:2 electrolyte), the GSSG desorption behavior was similar to that in Na₂SO₄ solution, thus exchanging Na⁺ with the larger NH₄⁺ ion did not affect the GSSG desorption from Al_2O_3 and $\text{Al}_2\text{O}_3\text{-NH}_2$. In contrast, for $\text{Al}_2\text{O}_3\text{-SO}_3\text{H}$, even a 100 mM NaCl concentration did not support GSSG desorption, indicating a stronger interaction of GSSG with $\text{Al}_2\text{O}_3\text{-SO}_3\text{H}$ than with Al_2O_3 and $\text{Al}_2\text{O}_3\text{-NH}_2$. In contrast, presence of either Na₂SO₄ or (NH₄)₂SO₄ enabled a concentration-dependent GSSG desorption from $\text{Al}_2\text{O}_3\text{-SO}_3\text{H}$ and 100 mM of these salts desorbed 68% and 63%, respectively, of the bound GSSG.

3.6. Reduction of the Disulfide Bond of Adsorbed GSSG. One GSSG molecule contains two glutathionyl (GS) moieties, which are connected by a disulfide bond (Figure 1). Reduction of GSSG with DTT will therefore generate two GSH molecules. This reduction allows to estimate whether one or both of the two GS moieties of one adsorbed GSSG molecule contributes to the binding to the particles, following the approach of Dringen et al.¹¹ Therefore, 0.1 vol % of the particles was preincubated for 30 min with 1 mM GSSG to bind GSSG, unbound GSSG was removed, and the particles were subsequently incubated for 60 min with ddH₂O or with 20 mM DTT in ddH₂O. The amount of particle adsorbed GS moieties

after incubation at nonreducing or reducing conditions (absence and presence of DTT, respectively) is shown in Figure 5A. For Al_2O_3 and $\text{Al}_2\text{O}_3\text{-NH}_2$ particles, about 75% of the initially bound GS-moieties was released by the DTT treatment compared to the nonreducing conditions. In contrast, DTT treatment did not liberate any GS moieties from GSSG that had been adsorbed to $\text{Al}_2\text{O}_3\text{-SO}_3\text{H}$ particles, suggesting that both GS moieties of GSSG are involved in interactions with the surface of $\text{Al}_2\text{O}_3\text{-SO}_3\text{H}$ -functionalized particles.

The ζ potential and IEP measurements were used to confirm the results of the DTT treatment and to provide information on the functional groups of adsorbed GSSG or of the particle surface that contributes to the electrokinetic particle properties. We therefore compared ζ potential and IEP of the particles without GSSG, after GSSG adsorption, and after GSSG adsorption and DTT treatment (Figure 5 B). For native Al_2O_3 particles, the GSSG adsorption shifted the IEP from 9.3 ± 0.1 to the more acidic 7.2 ± 0.1 , demonstrating the contribution of adsorbed GSSG to the electrokinetic particle properties. After DTT treatment, the IEP was shifted back to more basic 8.8 ± 0.1 , which correlated with the loss of GS moieties. However, the initial IEP of Al_2O_3 was not recovered, indicating that GS moieties are still attached to the particle surface. For $\text{Al}_2\text{O}_3\text{-NH}_2$ -functionalized particles, GSSG adsorption shifted the IEP similarly from 10.9 ± 0.3 to the slightly more acidic 9.5 ± 0.2 . After DTT treatment, the IEP of $\text{Al}_2\text{O}_3\text{-NH}_2$ -functionalized particles was found at 11.0 ± 0.1 , representing almost the IEP of untreated $\text{Al}_2\text{O}_3\text{-NH}_2$ particles. However, the ζ potential curve of the treated particles was between that of bare and GSSG-covered $\text{Al}_2\text{O}_3\text{-NH}_2$ -particles, which suggests presence of remaining GS moieties on the particle surface. For $\text{Al}_2\text{O}_3\text{-SO}_3\text{H}$ -functionalized particles, the IEP varied only slightly after GSSG adsorption and DTT treatment. In addition, no significant variation of the ζ potential curve was observed, suggesting that the $\text{-SO}_3\text{H}$ groups still dominate the electrokinetic properties of these particles, in correlation with the below-monolayer amounts of adsorbed GSSG on $\text{Al}_2\text{O}_3\text{-SO}_3\text{H}$ -functionalized particles.

4. DISCUSSION

GSSG adsorption is strongly affected by the surface functionalization of alumina particles as demonstrated by our data for particles with -NH_2 , -COOH , $\text{-SO}_3\text{H}$, and $\text{-PO}_3\text{H}_2$ functional groups, and the sensitive enzymatic cycling assay of GSSG allowed a precise analysis of the amounts of GSSG adsorbed and desorbed from the particles under various experimental conditions.

We observed high GSSG adsorption onto native alumina particles. As previously reported, the net negatively charged GSSG adsorbs effectively onto the positively charged alumina particles driven by electrostatic interactions between GSSG and alumina.¹¹ Functionalization of the alumina particles with -NH_2 groups introduced positively charged groups onto the surface, increased the particles IEP, and resulted in enhanced GSSG adsorption. This was observed although the net ζ potential was slightly lower for the -NH_2 -modified alumina particles when compared to native alumina particles, which may be due to the different pH values of the as-prepared and unbuffered solutions used for the measurements (pH 6.4 for -NH_2 -functionalized alumina and pH 4.8 for native alumina particles). The acidic functionalizations (-COOH , $\text{-PO}_3\text{H}_2$, and $\text{-SO}_3\text{H}$ functional groups) introduced a negative particle ζ potential, and according to an electrostatic interaction

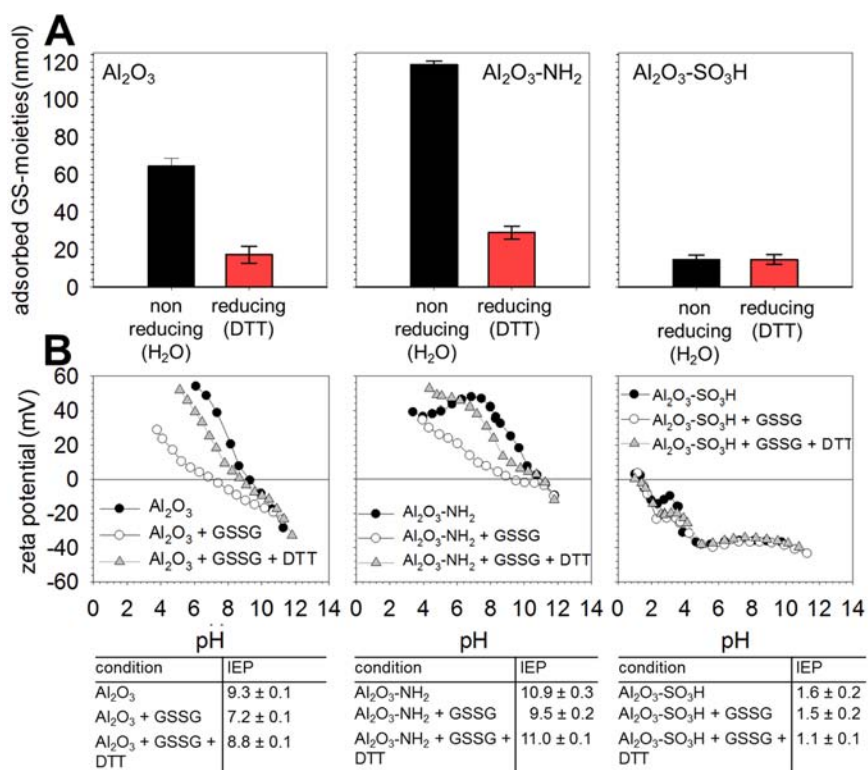


Figure 5. (A) Effects of dithiothreitol (DTT) on the GSSG adsorbed to Al₂O₃, Al₂O₃-NH₂- or Al₂O₃-SO₃H-functionalized particles: 0.1 vol % of the particles were preincubated for 30 min with 1 mM GSSG, the unbound GSSG was removed, and the particles were subsequently incubated for 60 min with ddH₂O or 20 mM DTT in ddH₂O. For the nonreducing conditions, the amount of adsorbed GSSG is considered to be not affected, while for the reducing conditions, it is assumed that exposure to DTT will have reduced all disulfide bonds in the adsorbed GSSG. The data represent the amount of GS-moieties in either GSSG or GSH that remained adsorbed on the particle surface during the main incubation and were finally released by 10 mM KOH. (B) Influence of the GSSG adsorption and DTT treatment on the ζ potential as function of the pH and the particles' IEP. The data represent means \pm standard deviation of three independent experiments.

approach, they lowered (Al₂O₃-SO₃H) or even prevented (Al₂O₃-COOH, -PO₃H₂) adsorption of net negatively charged GSSG to the particles (Figures 1 and 2). Unexpectedly, some GSSG adsorption was exclusively found on -SO₃H-functionalized alumina, although -COOH and -PO₃H₂-functionalized particles have almost the identical ζ potential. It was previously shown that protein adsorption on -SO₃H-functionalized alumina also varies from that of -COOH and -PO₃H₂-functionalized alumina particles, and an influence of the different acidity of the functional groups was suggested to be responsible for this effect.²² Indeed, -SO₃H groups have the lowest pK_a (pK_a = 1.53) value, and the deprotonated state is most stable compared to the -COOH (pK_a = 4.13) and -PO₃H₂ (pK_a = 2.16) groups at the pH of about 4.2 \pm 0.1,⁵¹ beneficial and necessary for interactions with the positively charged sites on GSSG. Milani et al. also reported different protein adsorption on -COOH and -SO₃H modified polystyrene particles and found that the adsorption of transferrin is stronger on -SO₃H modified particles than on -COOH modified particles.¹⁴ A further effect may derive from the close proximity (geminal configuration) of the positively charged amino and negatively charged carboxylate group in the GSSG molecule. The binding of GSSG via its positively charged amino group with a negatively charged particle surface group might be hindered if a second negatively charged particle surface group is nearby and repulses the carboxylate group of GSSG. Such an effect may particularly happen in the case of Al₂O₃-COOH, where the precursor molecule carries two vicinal carboxylate groups.

Native alumina, -NH₂-, and -SO₃H-functionalized alumina particles were investigated in detail to study the molecular mechanisms involved in their GSSG adsorption behavior. GSSG adsorption was rapid as demonstrated by maximal bindings that were achieved within 5 min, and the adsorption isotherms demonstrated that the GSSG adsorption was saturable. The Gibbs energy of adsorption ΔG_{ads}^0 estimated from the GSSG adsorption isotherms were in the range of typical values for electrostatic adsorption processes (<50 kJ/mol)⁵² and similar to those previously found for GSSG and GSH adsorption onto alumina.^{11,13} The negative values of ΔG_{ads}^0 which were almost identical for Al₂O₃, Al₂O₃-NH₂, or Al₂O₃-SO₃H particles, indicate an exergonic adsorption behavior of GSSG to all three types of particles, which thus appears in this regard to be rather independent of the surface functionalization.

That mainly electrostatic interactions are responsible for the adsorption of GSSG to the particle surface is further supported by the ability of salts to desorb GSSG from the three types of particles investigated. Nonetheless, independent of the particle surface chemistry, some GSSG remained adsorbed on the particles after salt application, which was not unexpected, as electrostatic interactions still occur at the highest ionic strengths used (Debye lengths are \approx 1 nm at 100 mM).⁵³ In addition, a contribution of nonelectrostatic interaction forces (e.g., hydrogen bonding) in GSSG-particle interaction cannot be totally excluded but is likely to play only a secondary role in the interaction between GSSG and the alumina particles investigated. Interestingly, the interaction between GSSG and

$-\text{SO}_3\text{H}$ -functionalized alumina seems to be more stable against exposure to different salt solutions than that of GSSG with native or $-\text{NH}_2$ -functionalized alumina, as the presence of NaCl, even in a concentration of 100 mM, was unable to desorb additional GSSG from the $-\text{SO}_3\text{H}$ -functionalized alumina compared to the respective salt-free control. This suggests a different binding mechanism and a potentially different orientation of GSSG on positively and negatively charged surfaces as discussed in the following.

The saturation of GSSG adsorption suggests that a limited number of adsorption sites for GSSG are available on the particle surface and excludes substantial multilayer formation by peptide-peptide interactions between GSSG and particle-adsorbed GSSG. The GSSG concentrations that enable maximal GSSG binding were transferred into the surface area occupied by one GSSG molecule (1.95 nm² per GSSG molecule on native alumina, 1.0 nm² on $-\text{NH}_2$ -functionalized alumina, and 4.0 nm² on $-\text{SO}_3\text{H}$ -functionalized alumina). The results for native alumina and $-\text{NH}_2$ -functionalized alumina are quite alike the projection areas calculated from a rigid structure of the GSSG molecule, maximal 1.55 nm² (side-on area) and minimal 1.0 nm² (end-on area), respectively (Figure S3).⁵⁰ Although GSSG is a flexible molecule and conformational changes are likely to influence the molecule size during adsorption,^{9,11} the strong correlation of the theoretical and experimentally determined GSSG adsorption area suggests that GSSG adsorbs in a side-on adsorption mode on native alumina particles and in an end-on adsorption mode on $-\text{NH}_2$ -functionalized alumina particles.

The approach estimates also which functional groups of the particles and the GSSG molecule can theoretically interact with each other. A surface area of 1.55 nm² on native alumina particles ($2.0 \pm 0.2 \text{ Al-OH/nm}^2$) contains about 3 Al-OH groups which could potentially interact with 1–3 of the 4 carboxylate groups of GSSG in side-on orientation. This is only possible when all Al-OH groups determined by potentiometric are sterically accessible and equivalent binding sites for the GSSG carboxylate groups. That may not be always the case, and GSSG is indeed suggested to bind, despite side-on orientation, with only 1–2 carboxylates of one GS moiety as discussed later. GSSG has a higher affinity for $-\text{NH}_2$ -functionalized alumina particles and is proposed to adsorb on these particles with its minimal projection area reaching higher surface packing than on native alumina particles. The concentration of $-\text{NH}_2$ groups per surface area is $<3.4 \text{ NH}_2/\text{nm}^2$ (although the IEP of these particles clearly demonstrates the presence of $-\text{NH}_2$ an exact quantification via elemental analysis was not achieved). A GSSG molecule that covers 1.0 nm² can contact thus maximally three $-\text{NH}_2$ groups. The suggested end-on adsorption mode of GSSG might promote that only 1–2 of the $-\text{COO}^-$ groups of GSSG interact with the particle surface. This assumption is further supported by the slightly lower adsorption enthalpy for $-\text{NH}_2$ -functionalized alumina compared to native or $-\text{SO}_3\text{H}$ functionalized particles, which is influenced by the number of functional groups/charge carriers interacting during adsorption.⁵⁴ Moreover, the results of the reduction of the disulfide bridges of bound GSSG on the particle surface by DTT suggest that GSSG interacts indeed with only one of its two GS moieties with native and $-\text{NH}_2$ -functionalized alumina particles (also previously suggested for native alumina).¹¹ On both, native and $-\text{NH}_2$ -functionalized particles, the reduction of the disulfide bridge removed $>50\%$ of the GS moieties which are not bound to the particle surface

(Figure 5). The loss of GS moieties even exceeds 50% indicating that some of the GSH moieties generated on the particles during the reduction of adsorbed GSSG will desorb from the particles consistent with the previous findings that binding of GSH is weaker on alumina surfaces than that of GSSG and bound GSH quickly desorbs from alumina to establish equilibrium between adsorbed and free GSH.^{11,13}

On $-\text{SO}_3\text{H}$ -functionalized alumina particles, the experimentally determined GSSG projection area (4.0 nm²/GSSG molecule) is higher than the maximal theoretical projection area of GSSG. This suggests that GSSG is not densely packed on the particle surface and some particle surface may remain uncovered. The repulsion between negatively charged $-\text{SO}_3^-$ groups of the particles and carboxylate groups of GSSG could be a driving force preventing a better coverage of the surface. Assuming that GSSG covers its maximal projection area (side-on, 1.55 nm²/GSSG molecule) on $-\text{SO}_3\text{H}$ -modified alumina ($4.6 \pm 0.2 \text{ SO}_3\text{H/nm}^2$), a GSSG molecule would occupy about seven $-\text{SO}_3\text{H}$ groups. Due to such a high availability of $-\text{SO}_3\text{H}$ groups per GSSG molecule, it is likely that both of the two protonated $-\text{NH}_3^+$ of the GSSG interact with deprotonated $-\text{SO}_3^-$ groups on the particle surface. This hypothesis is strongly supported by the results of the reduction of the disulfide bridges of bound GSSG on the particle surface by DTT, which does not lower the amount of adsorbed GS moieties on $\text{Al}_2\text{O}_3-\text{SO}_3\text{H}$. As each of the GS moiety of GSSG contains one $-\text{NH}_3^+$, that is likely to interact with the $-\text{SO}_3^-$ groups of the particle surface, the reduction of one molecule of adsorbed GSSG into two molecules of bound GSH will not lower the amount of adsorbed GS moieties from $-\text{SO}_3\text{H}$ -functionalized alumina. Illustration of hypothetical binding modes of GSSG on Al_2O_3 , $\text{Al}_2\text{O}_3-\text{NH}_2$, or $\text{Al}_2\text{O}_3-\text{SO}_3\text{H}$ -functionalized particles is given in Figure 6.

The electrokinetic analysis of the particles after GSSG adsorption and disulfide bridge reduction (Figure 5) supports the proposed adsorption behavior. Assuming that the surface is completely covered with GSSG in case of native and $-\text{NH}_2$ -

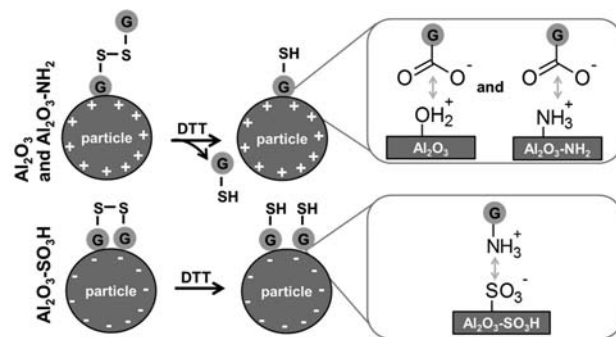


Figure 6. Illustration of hypothetical binding modes of GSSG on Al_2O_3 , $\text{Al}_2\text{O}_3-\text{NH}_2$, or $\text{Al}_2\text{O}_3-\text{SO}_3\text{H}$ -functionalized particles. GSSG contains two GS moieties that are connected by a disulfide bridge. Reduction of GSSG by DTT will generate two molecules of GSH. In case of Al_2O_3 and $\text{Al}_2\text{O}_3-\text{NH}_2$ about 75% GSH molecules are released by the DTT treatment and around 25% remain bound to the particle by electrostatic interactions between positively charged groups on the particle surface and negatively charged carboxylate groups of GSH. In case of $\text{Al}_2\text{O}_3-\text{SO}_3\text{H}$ particles, the DTT treatment does not liberate any GSH, and it is expected that both GS moieties are bound to the particle surface by interactions between negatively charged $-\text{SO}_3\text{H}$ groups on the particle surface and positively charged protonated $-\text{NH}_2$ groups of the GSSG.

functionalized alumina, only the functional groups of the adsorbed GSSG will determine the ζ potential and IEP, and the initial particle surface will lose its influence. For native and $-\text{NH}_2$ -functionalized alumina, GSSG adsorption shifted the particles IEP to more acidic values, which demonstrates the contribution of free carboxylate groups of GSSG to the establishment of the new IEP. Those carboxylate groups that contribute to the particle IEP are unlikely to be involved in binding between GSSG and the particle surface.

In addition, the ζ potential and IEP of native and $-\text{NH}_2$ -functionalized alumina after GSSG adsorption were not completely governed by negative carboxylate groups which would have led to a negatively charged and acidic IEP. This observation suggests a contribution of unbound protonated $-\text{NH}_3^+$ groups of GSSG to the electrokinetic properties. The increase of the IEP after DTT treatment confirms the release of GS moieties from native and $-\text{NH}_2$ -functionalized alumina. In contrast, in case of $-\text{SO}_3\text{H}$ -functionalized particles, the GSSG adsorption did not alter the IEP and pH-dependent ζ potential as expected by a substantial influence of the initial particle surface of $-\text{SO}_3\text{H}$ -functionalized alumina on the IEP and ζ potential due to only partial GSSG coverage. Due to their likely involvement in binding of GSSG to the $-\text{SO}_3\text{H}$ -functionalized alumina particles, the positively charged $-\text{NH}_3^+$ groups of GSSG do not significantly impact the electrokinetic particle properties, which should also not be affected by reduction of bound GSSG to GSH by DTT. Indeed, DTT treatment did not affect the ζ potential and only marginally the IEP of $-\text{SO}_3\text{H}$ -functionalized alumina particles that had been preincubated with GSSG.

CONCLUSIONS

The surface chemistry of colloidal alumina particles tailored with $-\text{NH}_2$, $-\text{COOH}$, $-\text{PO}_3\text{H}_2$, and $-\text{SO}_3\text{H}$ functional groups strongly affects the adsorption and the orientation of GSSG on the particle surface. Although electrostatic interactions are suggested as a main driving force for the GSSG adsorption, the type, concentration, and acidity/basicity of the functional surface groups, rather than just the ζ potential, have to be considered to predict and control GSSG adsorption. Our data suggest the following adsorption behavior of GSSG as function of the particle surface chemistry: GSSG adsorbs on positively charged native alumina in monolayer concentrations via the carboxylate groups of one of its GS moieties in a side-on orientation. GSSG has a higher affinity and denser surface packing on positively charged $-\text{NH}_2$ -functionalized alumina, binding in end-on orientation also via the carboxylate groups of one GS moiety. Among the acidic and negatively charged particles bearing $-\text{PO}_3\text{H}_2$, $-\text{COOH}$, and $-\text{SO}_3\text{H}$ groups, GSSG adsorbs exclusively onto $-\text{SO}_3\text{H}$ modified alumina. Here, GSSG is suggested to bind with both GS moieties via its two protonated amino groups and only partially covers the particle surface in a side-on orientation. These results represent a firm base for further studies on GSSG and peptide adsorption phenomena at physiological conditions or in biological fluids under competition with other peptides and proteins. Tailored particle surface functionalization might then be employed to control peptide and protein adsorption amount and orientation by a specific design of the materials surface chemistry and its functional groups.

ASSOCIATED CONTENT

Supporting Information

Isoelectric point of Al_2O_3 , $\text{Al}_2\text{O}_3-\text{NH}_2$, $\text{Al}_2\text{O}_3-\text{COOH}$, $\text{Al}_2\text{O}_3-\text{SO}_3\text{H}$, and $\text{Al}_2\text{O}_3-\text{PO}_3\text{H}_2$ after a 10 mM KOH treatment and GSSG projection areas. This material is available free of charge via the Internet at <http://pubs.acs.org>

AUTHOR INFORMATION

Corresponding Author

krezwana@uni-bremen.de

Author Contributions

^{||}These authors contributed equally.

Notes

The authors declare no competing financial interest.

ACKNOWLEDGMENTS

We thank the European Research Council for financial support within the BioCerEng, project no. 205509.

REFERENCES

- (1) Monopoli, M. P.; Aberg, C.; Salvati, A.; Dawson, K. A. *Nanotechnol.* **2012**, *7*, 779.
- (2) Vallee, A.; Humblot, V.; Pradier, C.-M. *Acc. Chem. Res.* **2010**, *43*, 1297.
- (3) Nel, A. E.; Maedler, L.; Velegol, D.; Xia, T.; Hoek, E. M. V.; Somasundaran, P.; Klaessig, F.; Castranova, V.; Thompson, M. *Nat. Mater.* **2009**, *8*, 543.
- (4) Helms, B.; van Baal, I.; Merckx, M.; Meijer, E. W. *ChemBioChem* **2007**, *8*, 1790.
- (5) Banerjee, I. A.; Yu, L.; Matsui, H. *Proc. Natl. Acad. Sci. U.S.A.* **2003**, *100*, 14678.
- (6) Costa, F.; Carvalho, I. F.; Montelaro, R. C.; Gomes, P.; Martins, M. C. L. *Acta Biomater.* **2011**, *7*, 1431.
- (7) Krauland, E. M.; Peelle, B. R.; Wittrup, K. D.; Belcher, A. M. *Biotechnol. Bioeng.* **2007**, *97*, 1009.
- (8) Cheng, R.; Feng, F.; Meng, F.; Deng, C.; Feijen, J.; Zhong, Z. *J. Controlled Release* **2011**, *152*, 2.
- (9) Soliman, W.; Bhattacharjee, S.; Kaur, K. *J. Phys. Chem. B* **2010**, *114*, 11292.
- (10) Thyparambil, A. A.; Wei, Y.; Latour, R. A. *Langmuir* **2012**, *28*, 5687.
- (11) Dringen, R.; Koehler, Y.; Derr, L.; Tomba, G.; Schmidt, M. M.; Treccani, L.; Colombi Ciacchi, L.; Rezwana, K. *Langmuir* **2011**, *27*, 9449.
- (12) Lopes, I. n.; Piao, L.; Stievano, L.; Lambert, J.-F. o. *J. Phys. Chem. C* **2009**, *113*, 18163.
- (13) Schmidt, M. M.; Koehler, Y.; Derr, L.; Treccani, L.; Rezwana, K.; Dringen, R. *J. Phys. Chem. C* **2012**, *116*, 23136.
- (14) Milani, S.; Baldelli Bombelli, F.; Pitek, A. S.; Dawson, K. A.; Rädler, J. *ACS Nano* **2012**, *6*, 2532.
- (15) Rothenstein, D.; Claasen, B.; Omiecienski, B.; Lammel, P.; Bill, J. *J. Am. Chem. Soc.* **2012**, *134*, 12547.
- (16) Joshi, S.; Ghosh, I.; Pokhrel, S.; Mädler, L.; Nau, W. M. *ACS Nano* **2012**, *6*, 5668.
- (17) Mirau, P. A.; Naik, R. R.; Gehring, P. *J. Am. Chem. Soc.* **2011**, *133*, 18243.
- (18) Seker, U. O. S.; Demir, H. V. *Molecules* **2011**, *16*, 1426.
- (19) Hoshino, Y.; Koide, H.; Urakami, T.; Kanazawa, H.; Kodama, T.; Oku, N.; Shea, K. J. *J. Am. Chem. Soc.* **2010**, *132*, 6644.
- (20) Basalyga, D. M.; Latour, R. A. *J. Biomed. Mater. Res., Part A* **2003**, *64A*, 120.
- (21) Meder, F.; Brandes, C.; Treccani, L.; Rezwana, K. *Acta Biomater.* **2013**, *9*, 5780.
- (22) Meder, F.; Daberkow, T.; Treccani, L.; Wilhelm, M.; Schowalter, M.; Rosenauer, A.; Maedler, L.; Rezwana, K. *Acta Biomater.* **2012**, *8*, 1221.

- (23) Wei, Y.; Latour, R. A. *Langmuir* **2009**, *25*, 5637.
- (24) Neouze, M.-A.; Schubert, U. *Monatsh. Chem.* **2008**, *139*, 183.
- (25) Larguezze, J.-B.; Kirat, K. E.; Morandat, S. *Colloids Surf, B* **2010**, *79*, 33.
- (26) Lazzara, T. D.; Behn, D.; Kliesch, T.-T.; Janshoff, A.; Steinem, C. *J. Colloid Interface Sci.* **2012**, *366*, 57.
- (27) Li, J.; Wang, J.; Gavalas, V. G.; Atwood, D. A.; Bachas, L. G. *Nano Lett.* **2002**, *3*, 55.
- (28) Li, H.; Li, Y.; Jiao, J.; Hu, H.-M. *Nat. Nanotechnol.* **2011**, *6*, 645.
- (29) Kossovsky, N.; Gelman, A.; Sponsler, E. E.; Hnatyszyn, H. J.; Rajguru, S.; Torres, M.; Pham, M.; Crowder, J.; Zemanovich, J.; Chung, A.; Shah, R. *Biomaterials* **1994**, *15*, 1201.
- (30) Hirrlinger, J.; Dringen, R. *Brain Research Reviews* **2010**, *63*, 177.
- (31) Schmidt, M.; Dringen, R. In *Advances in Neurobiology, Vol. 4: Neural Metabolism In Vivo*; Choi, I.-Y., Gruetter, R., Eds.; Springer: New York, 2012; Vol. 4, p 1029.
- (32) Park, H. A.; Khanna, S.; Rink, C.; Gnyawali, S.; Roy, S.; Sen, C. K. *Cell Death Differ.* **2009**, *16*, 1167.
- (33) Ellison, I.; Richie, J. P., Jr *Biochem. Pharmacol.* **2012**, *83*, 164.
- (34) Minich, T.; Riemer, J.; Schulz, J. B.; Wielinga, P.; Wijnholds, J.; Dringen, R. *J. Neurochem.* **2006**, *97*, 373.
- (35) Angeli, V.; Chen, H.; Mester, Z.; Rao, Y.; D'Ulivo, A.; Bramanti, E. *Talanta* **2010**, *82*, 815.
- (36) Monostori, P.; Wittmann, G.; Karg, E.; Túri, S. *J. Chromatogr., B* **2009**, *877*, 3331.
- (37) Noh, H.-B.; Chandra, P.; Moon, J. O.; Shim, Y.-B. *Biomaterials* **2012**, *33*, 2600.
- (38) Tietze, F. *Anal. Biochem.* **1969**, *27*, 502.
- (39) Saint-Denis, T.; Goupy, J. *Anal. Chim. Acta* **2004**, *515*, 191.
- (40) Dringen, R.; Kranich, O.; Hamprecht, B. *Neurochem. Res.* **1997**, *22*, 727.
- (41) Dringen, R.; Hamprecht, B. *J. Neurochem.* **1996**, *67*, 1375.
- (42) Gomma, G. K.; Wahdan, M. H. *Mater. Chem. Phys.* **1994**, *39*, 142.
- (43) Serro, A. P.; Degiampietro, K.; Colaço, R.; Saramago, B. *Colloids Surf, B* **2010**, *78*, 1.
- (44) ACD/Labs, version 5.0.0.184; Advanced Chemistry Development, Inc.: Toronto, ON, Canada, 2012; www.acdlabs.com.
- (45) PubChem Substance Database; National Center for Biotechnology Information: Bethesda, MD; <http://pubchem.ncbi.nlm.nih.gov/summary/summary.cgi?cid=44630308> (accessed December, 2012).
- (46) Pedretti, A.; Villa, L.; Vistoli, G. *J. Comput.-Aided Mol. Des.* **2004**, *18*, 167.
- (47) Baker, N. A.; Sept, D.; Joseph, S.; Holst, M. J.; McCammon, J. A. *Proc. Natl. Acad. Sci. U.S.A.* **2001**, *98*, 10037.
- (48) Humphrey, W.; Dalke, A.; Schulten, K. *J. Mol. Graphics* **1996**, *14*, 33.
- (49) Rezwani, K.; Meier, L. P.; Gauckler, L. J. *Langmuir* **2005**, *21*, 3493.
- (50) Maximal and minimal GSSG projection area estimated by the calculator plugin of Marvin version 5.4.0.0, ChemAxon (<http://www.chemaxon.com>) and a rigid conformation of GSSG extracted from the RCSB Protein Data Bank file (pdb ID: YCK1).
- (51) Lide, D. R. *CRC Handbook of Chemistry and Physics*, 75th ed.; CRC Press: Boca Raton, FL, 1994.
- (52) Bathen, D.; Breitbach, M. *Adsorption technology (German ed.)*; Springer: Berlin, 2001.
- (53) van Oss, C. J. *Interfacial Forces in Aqueous Media*, 2nd ed.; CRC press: Boca Raton, FL, 2006.
- (54) Baier, G.; Costa, C.; Zeller, A.; Baumann, D.; Sayer, C.; Araujo, P. H. H.; Mailänder, V.; Musyanovych, A.; Landfester, K. *Macromol. Biosci.* **2011**, *11*, 628.